

# STEAM REFORMING OF GLYCEROL OVER ALKALI-PROMOTED Co-Ni/Al<sub>2</sub>O<sub>3</sub> CATALYSTS

Chin Kui Cheng, Muhammad Syafiq Johari, Adesoji A. Adesina\*

Reactor Engineering & Technology Group,  
School of Chemical Engineering, The University of New South Wales, Sydney,  
New South Wales, Australia 2052

\*Email: [a.adesina@unsw.edu.au](mailto:a.adesina@unsw.edu.au)

## ABSTRACT

The steam reforming of glycerol over 5Co-10Ni/Al<sub>2</sub>O<sub>3</sub> catalysts promoted with Group I metals (2.5wt%) has been investigated. All catalysts were prepared by wetness co-impregnation of the metal nitrates and calcined at 873 K. Reforming reaction was carried out in a fixed-bed micro-reactor at 723 to 823 K under atmospheric pressure. BET surface area of the fresh catalysts decreased from 180 (for the unpromoted catalyst) to 125 m<sup>2</sup> g<sup>-1</sup> (for the Li-doped catalyst) although within the promoted catalysts, the area increased down the group attaining a maximum in the K-catalyst. Pore volume, however, remained insensitive to alkali addition. TPR profiles revealed that the alkali promotion decreased the reduction temperature for the various oxide phases in the Co-Ni/ Al<sub>2</sub>O<sub>3</sub> catalyst. Reforming runs revealed that H<sub>2</sub>:CO<sub>2</sub> ratio (2.30 to 2.40) on all catalysts were in agreement with stoichiometric expectation (2.33) at 823 K but gradually increased with decreasing temperature. The K-promoted catalyst gave the best activity. All promoters, with the exception of Cs, reduced the activation energy for H<sub>2</sub> and CO<sub>2</sub> production. Indeed, a compensation effect was observed within the Group I metals with different isokinetic temperatures for the pairs, H<sub>2</sub> and CO<sub>2</sub> as well as for CO and CH<sub>4</sub>. This suggests that the two pairs of products were most likely formed via different reaction pathways. In particular, while H<sub>2</sub> and CO<sub>2</sub> were primary products from the reforming reaction, CO and CH<sub>4</sub> arose from secondary hydrogenolysis of glycerol. Post-reaction characterisation of the used catalysts indicated that the superior activity of the K-promoted catalyst was probably due to stronger glycerol adsorption and hence, higher carbon deposition. The latter was, however, completely removable via TPR-TPO cycle which itself implicated the existence of at least two types of carbon deposits – a carbonaceous pool inert to H<sub>2</sub> and another reactive with both O<sub>2</sub> and H<sub>2</sub>.

## INTRODUCTION

Decreasing fossil fuel reserves and the resulting escalating oil price along with demand for increased dependency on renewable energy sources have combined to accelerate the development of new processes to convert biowaste to energy and valuable commodity chemicals. It is in this respect that the conversion of glycerol to synthesis gas has attracted increasing research attention. Glycerol is a waste by-product of biodiesel synthesis from the transesterification of non-edible oils with alcohol.

Hydrogen production from steam reforming of glycerol may be written:



The gas phase reforming process is strongly endothermic (cf. Eqn (2)) and the stoichiometry suggests that it will be favoured by low pressure, high temperatures and stoichiometrically excess steam to achieve higher conversion of glycerol to hydrogen (Pagliaro & Rossi, 2008; Adhikari *et al.*, 2007).

$$\Delta H_{GSR}(T) = \Delta H_{298} + 86.94 + 0.144T - 8.233 \times 10^{-5} T^2 + 6.50 \times 10^{-9} T^3 \quad (2)$$

where the standard heat of reaction at 298 K,  $\Delta H_{298} = 122.9 \text{ kJ mol}^{-1}$ . Thus, many studies have employed temperature above 773 K for producing hydrogen at atmospheric pressure using a feed steam-to-glycerol molar ratio (STGR) of 9:1 (Barbaro & Bianchini, 2009). These conditions will also minimize the production of methane and inhibited the formation of carbon. The possible side-reactions, namely;

*Glycerol decomposition:*



$$\text{with } \Delta H_{Gly.decomp}(T) = \Delta H_{298} + 205.64 + 0.19T - 2.27 \times 10^{-4} T^2 + 1.15 \times 10^{-7} T^3 \quad (4)$$

where  $\Delta H_{298} = 246.1 \text{ kJ mol}^{-1}$ .

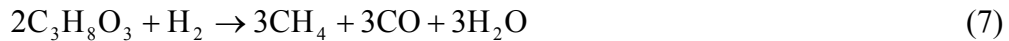
*Reverse water-gas shift (RWGS) reaction:*



$$\text{having } \Delta H_{RWGS}(T) = \Delta H_{298} + 39.47 + 0.016T - 4.68 \times 10^{-5} T^2 + 3.61 \times 10^{-8} T^3 \quad (6)$$

where  $\Delta H_{298} = 41. \text{ kJ mol}^{-1}$ .

*Hydrogenolysis reaction:*



$$\text{with } \Delta H_{Gly.hydrogenolysis}(T) = \Delta H_{298} - 607.85 - 0.02T - 1.545 \times 10^{-5} T^2 + 1.57 \times 10^{-8} T^3 \quad (8)$$

where  $\Delta H_{298} = -623.76.1 \text{ kJ mol}^{-1}$  are also thermodynamically favoured.

Dumesic group (Simonetti *et al.*, 2007; Kunkes *et al.*, 2009) have indicated that the mechanism of aqueous phase reforming (APR) at high pressures (3 MPa and 553 K) may be similar to that under atmospheric steam reforming conditions. However, metal leaching from the solid catalyst as well as solid-liquid separation issues following the reaction are significant disincentives. Noble metals reportedly exhibited better activities than other transition metals but the high cost of the Pt-group warrants closer examination of cheaper catalyst formulation using for example doping with known promoters in other hydrocarbon steam reforming operations. Product ratio, selectivity and catalyst stability may also benefit from such modifications. In this study, we investigate the performance of Co-Ni/Al<sub>2</sub>O<sub>3</sub> catalysts promoted with alkali metals (lithium, sodium, potassium and cesium) for glycerol steam reforming in a fixed-bed reactor over the temperature range 723-823 K at atmospheric pressure. Ni-based catalyst is an established hydrocarbon steam reforming operative while alkali promotion purportedly imparts anticoking resistance and/or stability augmentation (Hardiman *et al.*, 2004).

## EXPERIMENTAL

### Catalyst Preparation

Promoted Co-Ni/Al<sub>2</sub>O<sub>3</sub> catalysts were prepared in the ratio 2.5X:5Co:10Ni:77.5Al<sub>2</sub>O<sub>3</sub> (X = Li, Na, K, Cs) using the wetness impregnation technique. Metal nitrate precursors

were initially prepared based on the required amount needed to give the desired metal loading. These nitrate precursor solutions were gently added to a pre-weighed thermally treated  $\gamma$ - $\text{Al}_2\text{O}_3$ . Ultrapure water was then added to the  $\text{Al}_2\text{O}_3$  mixture. Stirring was done using autotitrator to ensure that the solution was homogeneously mixed. The slurry mixture was then left overnight in a furnace at 403 K to remove moisture and other volatile compounds. Calcination was done on the dried catalyst at 873 K for a period of 4 hours using a heating rate of 5 K  $\text{min}^{-1}$  from room temperature. The calcined catalyst was then crushed and sieved to 140-250  $\mu\text{m}$  particles for further use.

### **Catalyst Characterization**

$\text{N}_2$  adsorption-desorption measurements were used to determine the surface area, pore properties of the catalysts. Thermogravimetric analysis (TGA) of the calcination process was performed using a ThermoCahn TG 2121 unit containing 70-80 mg of the dried catalyst sample.  $\text{H}_2$  temperature-programmed reduction (TPR) runs were conducted on the calcined catalysts at a ramp rate of 5 K  $\text{min}^{-1}$  to 973 K and holding at this temperature for 2 hours, followed by cooling to ambient temperature in a  $\text{N}_2$  blanket in order to locate reducible solid oxide temperature peaks and determine their reduction kinetics. Complementary qualitative solid crystalline phase identification was also provided via X-ray diffraction measurements using a Philip X'Pert system equipped with Ni-filtered  $\text{CuK}\alpha$  ( $\lambda = 1.542 \text{ \AA}$ ) at 40 kV and 30 mA. A Total Organic Carbon (TOC) Analyzer 5000A coupled to a Shimadzu Solid Sample Module SSM-5000A was used to measure organic carbon content in the used catalyst specimens.

### **Catalyst Activity Evaluation**

The steam reforming of glycerol was conducted in a fixed-bed reactor at atmospheric pressure over 723-823 K. The reactor was a 490 mm long stainless steel tube (10 mm i.d). A 3-mm o.d. stainless steel thermocouple was positioned axially in the catalyst bed to measure the reaction temperature. Quartz wool (10mm thickness) was used to support the catalyst bed at both ends inside the tube. The quartz wool was placed 140 mm from the bottom of the tube. The exposed sections of reactor outside the tubular furnace were covered with kaowool to minimize temperature variation. About 0.270 g of the catalyst was placed above the quartz wool support. Prior to the activity test, the catalyst was reduced with 50  $\text{ml min}^{-1}$   $\text{H}_2$  at 873 K for 2 h. Water/glycerol mixture at a molar ratio of 6.25:1 was then injected by a syringe pump at 180  $\text{ml min}^{-1}$  into a vaporiser at 773 K before being passed over the catalyst bed. The catalyst activity was evaluated at 723, 773 and 823 K. The reactor exit stream was passed through a ice condenser to remove unused steam and non-condensable gases were sent to a drierite ( $\text{CaSO}_4$ ) bed prior to GC analysis. The latter is a Shimadzu GC 8A model equipped with a thermal conductivity detector and Haysep DB column with the isothermal operation at 333 K.

## **RESULTS AND DISCUSSION**

### **Catalyst Characterization**

Table 1 displays the physical attributes of the catalysts. It is evident that addition of the alkali promoters decreased the surface area and increased average pore size although there appeared to be no discernible change in the prove volume. These observations are

indicative of the intricate homogeneous mixing of the alkali ions with the support matrix. The changes in both BET area and pore size seemed to correlate with both ionic radius and electropositivity of the promoter.

Table 1: BET surface area and pore volume of catalysts

Catalyst	Surface Area ( $\text{m}^2 \text{g}^{-1}$ )	Pore Volume ( $\text{cm}^3 \text{g}^{-1}$ )	Pore Size ( $\text{\AA}$ )
Co-Ni/ $\text{Al}_2\text{O}_3$	180	0.59	131
Li-Co-Ni/ $\text{Al}_2\text{O}_3$	125	0.58	188
Na-Co-Ni/ $\text{Al}_2\text{O}_3$	139	0.48	139
K-Co-Ni/ $\text{Al}_2\text{O}_3$	166	0.58	140
Cs-Co-Ni/ $\text{Al}_2\text{O}_3$	162	0.55	136

The XRD patterns of the catalysts are all similar with no peaks for the alkali oxides ( $\text{X}_2\text{O}$ ) and hence, Figure 1 shows only the diffractogram for the Co-Ni/ $\text{Al}_2\text{O}_3$  catalyst. The absence of the alkali oxide phase may be due to relatively low concentration used. The pattern revealed large peaks for  $\text{CoAl}_2\text{O}_4$  ( $2\theta = 36.7^\circ$ ) and  $\text{NiAl}_2\text{O}_4$  at  $37^\circ$  and  $44.8^\circ$ . The small peaks are attributed to  $\text{NiCo}_2\text{O}_4$  at  $31^\circ$  and  $36.6^\circ$ ,  $\text{Co}_3\text{O}_4$  at  $31.2^\circ$  and  $36.8^\circ$ ,  $\text{NiO}$  at  $44.5^\circ$  and  $\text{NiAl}_2\text{O}_4$  at  $59.1^\circ$ . The TGA profiles for the catalysts are presented in Figure 2. The reduction of the unpromoted and promoted catalysts showed three peaks at different temperatures. The first peak at temperature range of 430 to 490 K corresponds to the reduction of  $\text{Ni}^{3+}$  ( $\text{Ni}_2\text{O}_3$ ) to  $\text{Ni}^{2+}$  or Ni where this compound was undetected via XRD measurement due to its amorphous nature [5]. The second peak at 570 to 640 K may be ascribed to the reduction of  $\text{Co}_3\text{O}_4$  and  $\text{NiO}$  to  $\text{CoO}$  and Ni respectively. The third peak represents the reduction of metal aluminate phases consisting of  $\text{CoAl}_2\text{O}_4$  and  $\text{NiAl}_2\text{O}_4$ . The addition of promoter appeared to lower the reduction peak temperature of the oxide phases with exception of the first peak.

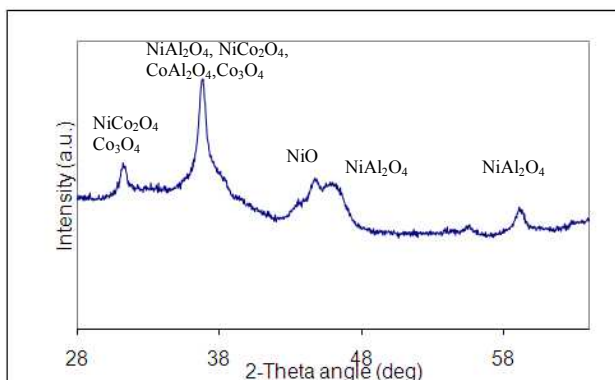


Figure 1: XRD for freshly calcined Co-Ni/ $\text{Al}_2\text{O}_3$

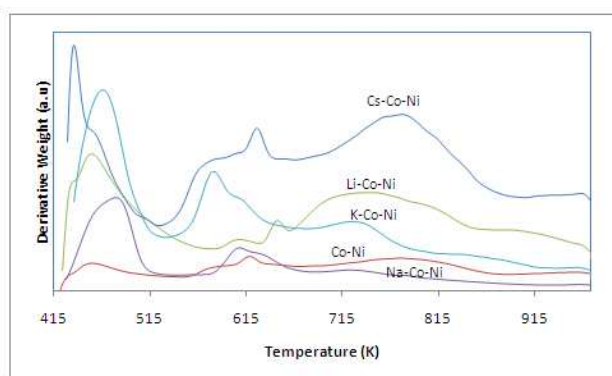


Figure 2: TPR profiles of all fresh catalysts

## Reaction Analysis

Figure 3 shows that glycerol conversion increased with temperature for all catalysts. Arrhenius treatment of the associated production rate for each species (typical plot shown in Fig. 4) yielded the activation energy,  $E_a$ , and frequency factor,  $A$ , estimates provided in Table 2. It is evident from these values that alkali promotion lowered the activation energy for all products compared with that for the undoped Co-Ni catalyst, indicating a change in the electronic environment of the active site. For both  $\text{H}_2$  and

CO<sub>2</sub>, the reduction in E<sub>a</sub> was maximum in the K-catalyst and decreased in the order, K>Na>Li>Cs ≈ unpromoted Co-Ni catalyst. The drop in activation energy for secondary products, CO and CH<sub>4</sub>, however, exhibited a different pattern. The E<sub>a</sub> was smallest for the Li-promoted catalyst for CO rate while for CH<sub>4</sub>, the Na-catalyst gave the lowest E<sub>a</sub> value. Since rates for CO and CH<sub>4</sub> increased in the same direction, it seems that neither steam reforming nor Fischer-Tropsch type reaction occurred to any appreciable extent during glycerol reforming. Indeed, the rate data point to the thermodynamically favourable glycerol hydrogenolysis as the more probable route for CO and CH<sub>4</sub> formation.

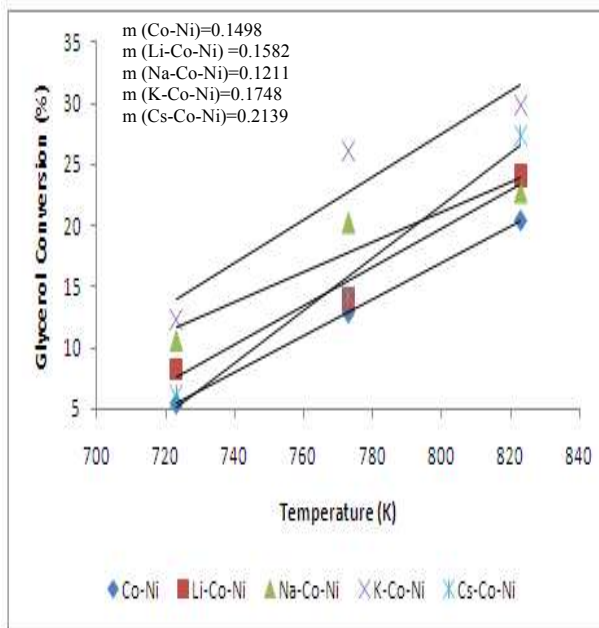


Figure 3: Glycerol conversion over all catalysts.

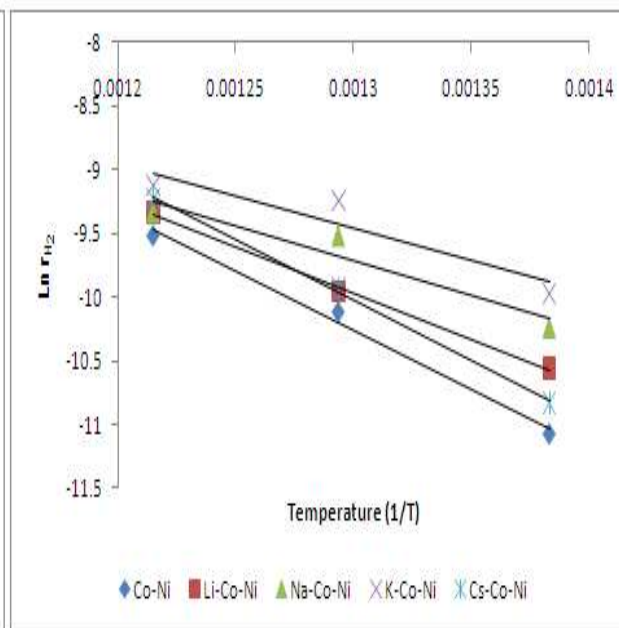
Figure 4: Arrhenius plot for H<sub>2</sub>

Table 2: Activation Energy and Frequency Factor of the product species

Catalysts	Product	Activation Energy (kJ mol <sup>-1</sup> )	Frequency Factor (mol g <sup>-1</sup> s <sup>-1</sup> )
Co-Ni	H <sub>2</sub>	77.07	32.06
	CO <sub>2</sub>	87.79	62.03
	CO	27.33	3.69E-3
	CH <sub>4</sub>	134.45	5247
Li-Co-Ni	H <sub>2</sub>	60.44	3.19
	CO <sub>2</sub>	67.84	3.89
	CO	23.08	2.09E-3
	CH <sub>4</sub>	78.52	0.95
Na-Co-Ni	H <sub>2</sub>	45.31	0.39
	CO <sub>2</sub>	48.33	0.27
	CO	30.1	7.04E-4
	CH <sub>4</sub>	69.63	0.32
K-Co-Ni	H <sub>2</sub>	42.80	0.34
	CO <sub>2</sub>	45.12	0.21
	CO	29.52	4.29E-3
	CH <sub>4</sub>	101.74	110.67

Cs-Co-Ni	H <sub>2</sub>	79.46	59.12
	CO <sub>2</sub>	83.34	43.71
	CO	54.11	0.22
	CH <sub>4</sub>	107.12	105.17

The correlation between activation energy,  $E_a$ , and the frequency factor,  $A$ , can also provide useful insights into the reaction analysis if the relation,

$$\ln A_j = aE_{a_j} + b \quad (9)$$

is satisfied as exemplified by the plots shown in Figure 5 for each species across all 5 catalysts with R-squared values greater than 0.99. Eqn (9) implicates the possibility of a compensation effect and has been invoked as a justification for common mechanism either for, a series of reactions over the same catalyst, or a specified reaction over a class of catalysts (Zhang et al. 2005; Bond, 1999; Wootsch & Paal 2002). In order to determine the validity of the associated isokinetic phenomenon, the criterion recommended by Liu & Guo (2001) was also derived as:

$$\Delta G^\ddagger = \left( \frac{1}{a} - RT \right) \ln \left( \frac{Ah}{k_B T} \right) + b \quad (10)$$

where  $k_B$ ,  $h$  and  $R$  are Boltzmann, Planck and gas constant respectively.  $\Delta G^\ddagger$  is the Gibbs free energy for the associated transition state complex during the individual product formation and used to evaluate the Arrhenius parameters. As may be seen from Figure 6, the present data produced an excellent fit with isokinetic temperature,  $T_{iso}$ , values of 1200 K (for H<sub>2</sub> and CO<sub>2</sub>) and 600 K (for CO and CH<sub>4</sub>) on all catalysts.

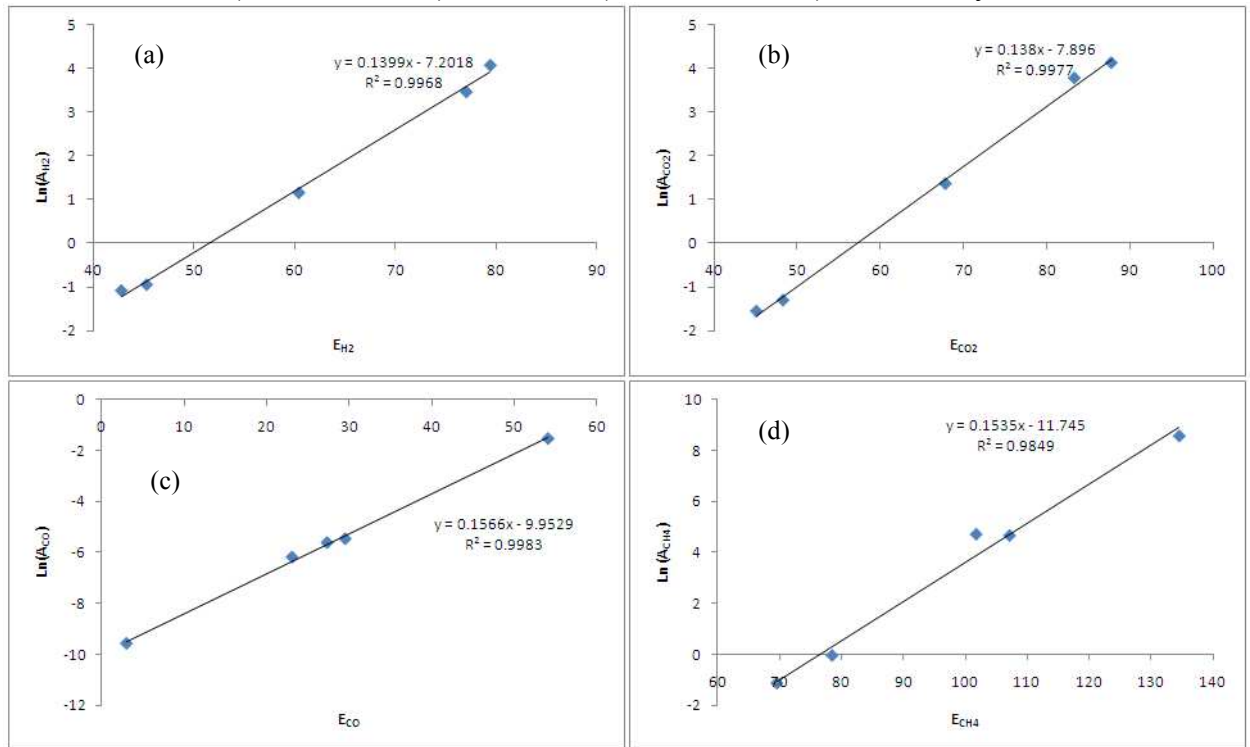


Figure 5: Proof of compensation effect within the class of catalysts (a) H<sub>2</sub>, (b) CO<sub>2</sub>, (c), CO and (d) CH<sub>4</sub>

This analysis further lends credence to the proposition that H<sub>2</sub> and CO<sub>2</sub> were the primary products formed via a different pathway from CO and CH<sub>4</sub> produced from the side-reaction, glycerol hydrogenolysis.

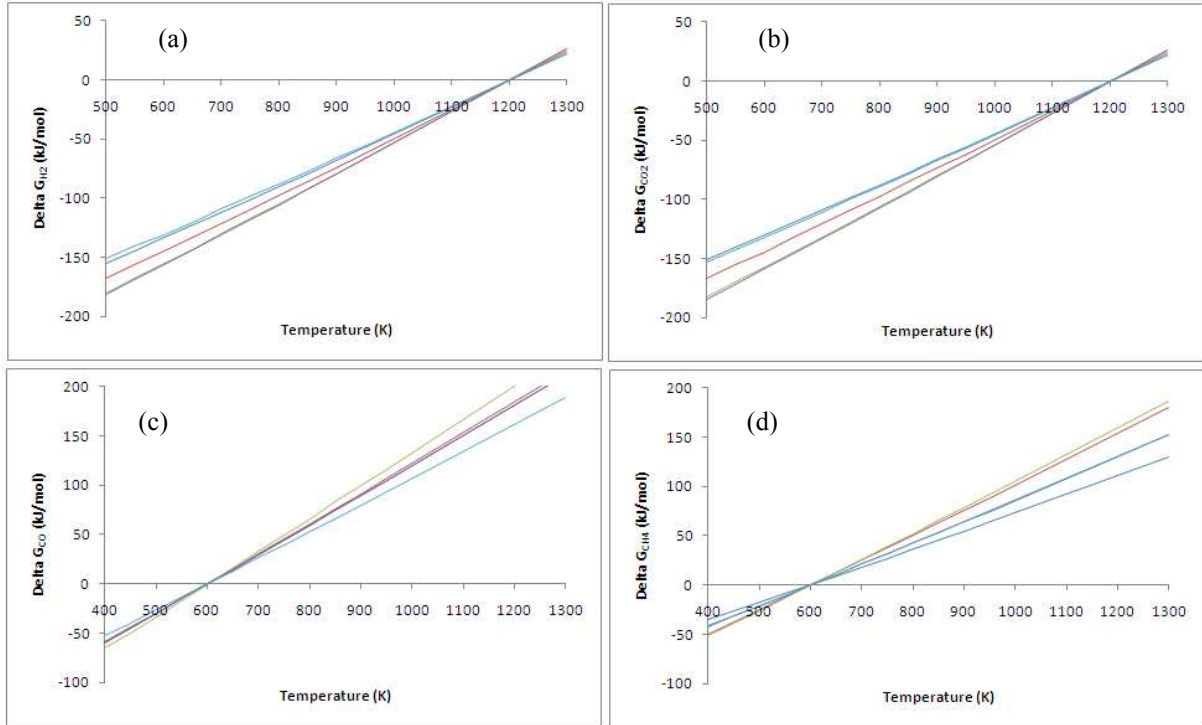


Figure 6: Isokinetic plots for (a) H<sub>2</sub>, (b) CO<sub>2</sub>, (c) CO and (d) CH<sub>4</sub>

### Product Ratio and Selectivity

Figure 7 shows that product ratio is dependent on temperature. The H<sub>2</sub>:CO<sub>2</sub> ratio decreased with temperature while the H<sub>2</sub>:CO ratio increased almost monotonically with temperature. At a given feed composition, the product ratio between any two species, i and j, P<sub>ij</sub>, may be given as:

$$P_{ij} = \frac{A_i}{A_j} e^{-(E_i - E_j)/RT} \quad (11)$$

Thus, decreasing H<sub>2</sub>:CO<sub>2</sub> ratio with temperature is consistent with the data in Table 2 where  $(E_{H_2} - E_{CO_2})$  is negative for all catalysts while the trend in H<sub>2</sub>:CO also agreed with  $(E_{H_2} - E_{CO}) > 0$ . Similarly, both H<sub>2</sub>:CH<sub>4</sub> and CO:CH<sub>4</sub> ratios decreased with temperature since  $(E_{H_2} - E_{CH_4})$  and  $(E_{CO} - E_{CH_4})$  are both less than zero.

The selectivity of a product, i, S<sub>i</sub>, defined;

$$S_i = \frac{r_i}{\sum_i r_i} \quad i = H_2, CO_2, CH_4 \text{ and CO} \quad (12)$$

The product selectivity for the catalysts is shown as bar plots in Figures 8(a-d) at various temperatures. It is clear that H<sub>2</sub> and CO<sub>2</sub> selectivities increased with temperature on all catalysts in agreement with the endothermic nature of the reforming reaction. The highest selectivities were observed on the Na- and K-promoted catalysts. CO selectivity

on the other hand decreased with temperature on all catalysts except for the K-promoted sample where it was in fact at its lowest value.  $\text{CH}_4$  selectivity was, however, highest on the K-catalyst when compared with other catalysts. Additionally, at 773 K it exhibited maximum selectivity – the same temperature where CO experienced the lowest selectivity. It would therefore seem that reverse water gas shift reaction was probably more significantly favoured on the K-catalyst.

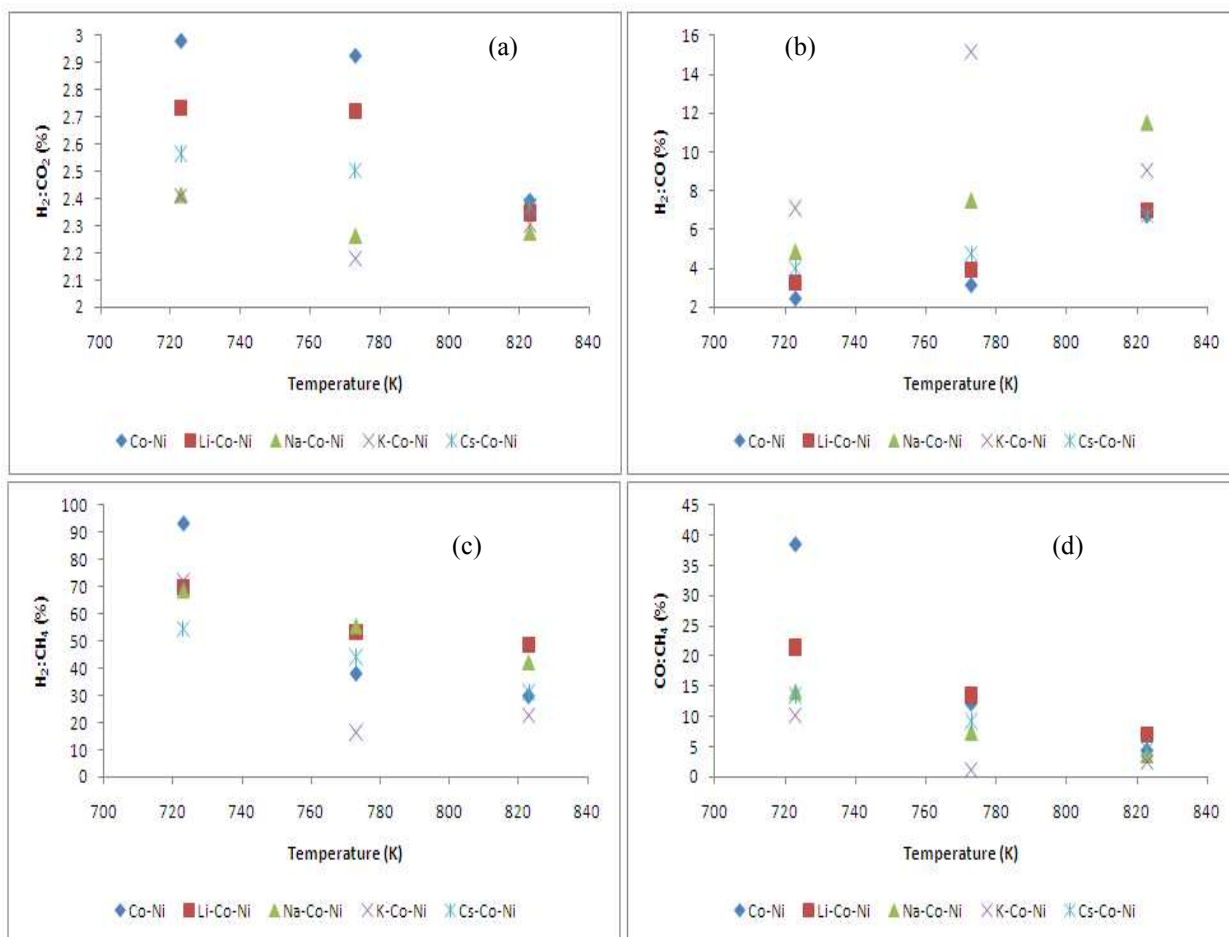


Figure 7: Product ratio at different temperatures for (a)  $\text{H}_2:\text{CO}_2$ , (b)  $\text{H}_2:\text{CO}$ , (c)  $\text{H}_2:\text{CH}_4$ , (d)  $\text{CO}:\text{CH}_4$

### Characterization of Used Catalysts

Post-reaction examination of the catalysts revealed a general reduction in BET areas for all catalysts compared to the corresponding fresh specimens as seen from Figure 9a. However, the trend with temperature is mixed. While the BET area of the used unpromoted Co-Ni catalyst increased with temperature, the opposite effect was witnessed on the K-doped catalyst and there was no clear change in this property for both Li and Cs promoted catalysts. The trend may have been compounded with the presence and amount of total organic carbon present on each catalyst and therefore not

necessarily due to thermally induced structural changes. Indeed, Figure 9b shows that only the K-catalyst had substantially more carbon deposition than the unpromoted

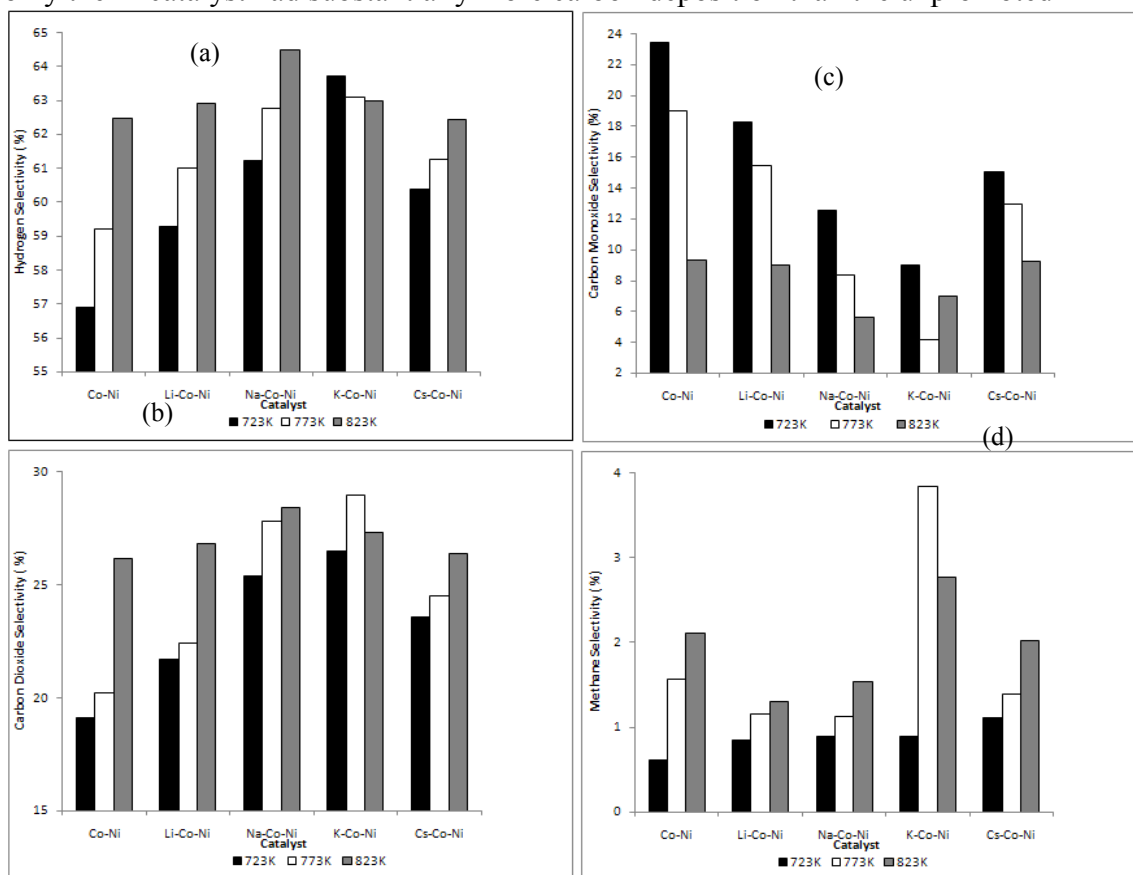


Figure 8: Selectivity at different temperatures for (a) H<sub>2</sub>, (b) CO<sub>2</sub>, (c) CO, (d) CH<sub>4</sub>

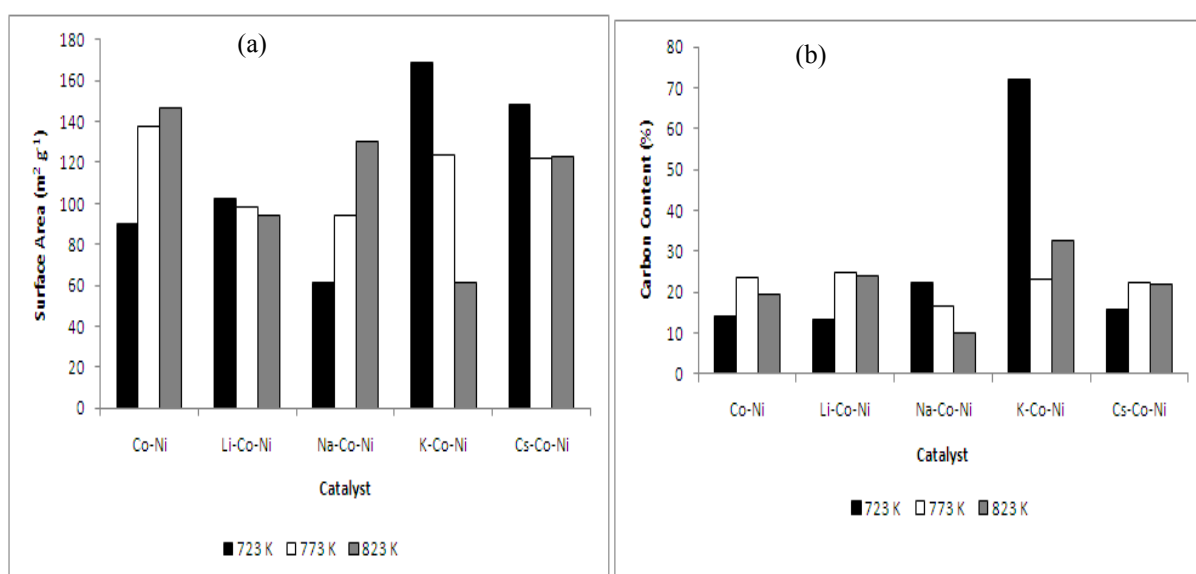


Figure 9: (a) BET surface area for used catalysts at different temperatures, (b) TOC analysis of unpromoted and promoted catalysts

catalyst. The used catalysts were also subjected to H<sub>2</sub> TPR followed by TPO (in air) using the same procedure as for the fresh specimens. As may be seen from Table 4, the percent weight change was highest on the K-catalyst consistent with the independent TOC analysis results (cf. Figure 9b). In particular, all catalyst contained a significant amount of carbonaceous deposit that was unreactive with H<sub>2</sub> but could only be removed by O<sub>2</sub>.

Table 4: Percent weight change for catalysts used at T = 823 K

Catalysts	Percent of weight change (%)		Total percent of weight change (%)
	TPR	TPO	
Co-Ni	6.15	16.13	22.28
Li-Co-Ni	7.69	22.95	30.64
Na-Co-Ni	11.29	25.57	36.86
K-Co-Ni	15.39	28.57	43.96
Cs-Co-Ni	9.68	17.54	27.22

## CONCLUSIONS

The present study has shown that addition of Group I metals to alumina-supported Co-Ni catalyst for glycerol steam reforming improved activity with K and Na promoters giving the best results. Product ratio dependency on temperature was however similar for all catalysts. Reaction analysis revealed that H<sub>2</sub> and CO<sub>2</sub> were the primary products from the reforming reaction while CO and CH<sub>4</sub> arose from glycerol hydrogenolysis with H<sub>2</sub>. The class of promoted catalysts was characterised by a compensation effect and the associated isokinetic temperature further lend credence to the proposition of different reaction pathways for the product pairs. Spent catalysts contained similar types of carbon deposits and the amount seemed to correlate linearly with the enhancement seen in catalytic activity suggesting that the improvement was most likely due to stronger glycerol adsorption upon alkali promotion.

## REFERENCES

- Adhikari, S, Fernando, SD; Haryanto, A, 2007, 'Production of hydrogen by steam reforming of glycerin over alumina-supported metal catalysts', *Catalysis Today* 129, pp355-364
- Barbaro, P, & Bianchini, C, 2009, *Catalysis for Sustainable Energy Production*, Wiley-VCH, 2009
- Bond G, 1999, 'Kinetics of alkane reactions on metal catalysts: activation energies and the compensation effect'. *Catal Today* vol 49, pp41-48.
- Hardiman, KM, Ying TT, Adesina, AA, Kennedy, EM & Dlugogorski, BZ, 2004, 'Performance of a Co-Ni catalyst for propane reforming under low steam-to-carbon ratios'. *Chem. Eng. J.* vol 102, pp119-124.
- Kunkes, EL, Soares, RR, Simonetti, DA & Dumesic, JA, 2009 'An integrated catalytic approach for the production of hydrogen by glycerol reforming coupled with water-gas shift', *Applied Catalysis B: Environmental*, vol 90, pp 693 – 698.
- Liu, L & Guo, QX 2001, 'Isokinetic relationship, isoequilibrium relationship, and Enthalpy-Entropy compensation', *Chemical Reviews*, vol. 101, pp. 673-695.

- Mile, B, Stirling, D, Zammit, MA., Lovell, A & Webb, MJ, 1990, 'TPR studies of the effects of preparation conditions on supported nickel and ruthenium catalysts, *Appl. Catal.*, 55, 1990, pp179-198
- Pagliari, M & Rossi, M, 2008, 'The future of glycerol: new uses of a versatile raw material', *Catalysis Applications*, Royal Society of Chemistry.
- Simonetti, DL, Kunkes, EL, & Dumesic, JA, 2007, 'Gas-phase conversion of glycerol to synthesis gas over carbon-supported platinum and platinum-rhenium catalysts', *Journal of Catalysis* 247, pp298-306
- Wootsch, A & Paal, Z 2002, 'Reactions of n-Hexane on Pt catalysts: reaction mechanism as revealed by hydrogen pressure and compensation effect'. *J Catal* vol 205, pp 86-96.
- Zhang J, Xu H, & Li W 2005, 'Kinetic study of NH<sub>3</sub> decomposition over Ni nanoparticles: the role of La promoter, structure sensitivity and compensation effect'. *Appl Catal A: General*, vol 296, pp257-267.

#### **BRIEF BIOGRAPHY OF PRESENTER**

Chin Kui Cheng is currently a PhD student from University of New South Wales. He is on study leave from Universiti Malaysia Pahang, Kuantan Malaysia. His research interest is in glycerol reforming reactions.